Nanoscale

DNA Hydrogel Delivery Vehicle for Light-triggered and Synergistic Cancer Therapy

Journal:	*Nanoscale*
Manuscript ID:	NR-COM-02-2015-000858.R1
Article Type:	Communication
Date Submitted by the Author:	06-Apr-2015

Complete List of Authors:	Song, Jaejung; Pohang University of Science and Technology, School of Interdisciplinary Bioscience and Bioengineering Im, Kyuhyun; Samsung Advanced Institute of Technology, Hwang, Sekyu; Pohang University of Science and Technology, Chemistry Hur, Jaehyun; Gachon University, Department of Chemical and Biological Engineering Nam, Jutaek; Pohang University of Science & Technology, Chemistry Ahn, G-One; Pohang University of Science and Technology, Division of Integrative Biosciences and Biotechnology Hwang, Sungwoo; Samsung Advanced Institute of Technology, Kim, Sungjee; Pohang University of Science and Technology, Chemistry Park, Nokyoung; Myongji University, Department of Chemistry

Journal Name

RSCPublishing

COMMUNICATION

DNA Hydrogel Delivery Vehicle for Light-triggered and Synergistic Cancer Therapy

Cite this: DOI: 10.1039/x0xx00000x

Jaejung Song,[a] Kyuhyun Im,[b] Sekyu Hwang,[c] Jaehyun Hur,[d] Jutaek Nam,[c] G-One Ahn[e], Sungwoo Hwang,[b] Sungjee Kim[*a,c] and Nokyoung Park[*f]

Received 00th January 2012,
Accepted 00th January 2012

DOI: 10.1039/x0xx00000x

www.rsc.org/

DNA hydrogel is reported as a delivery vehicle for gold nanorod and doxorubicin. The two photothermal and chemo cancer agents were co-loaded using electrostatic and DNA binding interactions, respectively. Light-triggered and highly synergistic combination cancer therapy was demonstrated at cellular and also at animal model.

Gold nanostructures of which surface plasmon resonance (SPR)[1] tuned at near-infrared (NIR) wavelengths such as nanorods,[2] nanoshell,[3] and nanocages,[4] have demonstrated the potential for many deep-tissue penetrating biomedical applications that include photothermal therapy, Raman imaging and radio-sensitization. Gold nanorods (AuNRs) have been widely used for photothermal effect because of their relative simplicity in synthesis, the strong local heating upon NIR irradiation that cannot be paralleled by conventional organic dye-based agents, and resistance against photobleaching.[5] Typically, many photothermal agents including gold nanoparticles (NPs) can carry a number of small molecules by the flexible surface functionalities for efficient drug delivery.[6] However, most of AuNR surfaces are covered by surfactants such as cetyltrimethylammonium bromide (CTAB) which is essential for the NR morphology control but lacks conjugation capability. As the result, it is difficult to attain a AuNR hybrid system that integrates conventional anticancer agents in the proximity of AuNR and permits multimodal thermo-chemo combination cancer therapy.[7] To achieve maximal synergistic effect by combination therapy, the proximity between the two agents is crucial.[8] In cases where chemo-agents were combined with NPs by physical mixtures[7a, 7b] or by loosely bound conjugates through hydrophobic interactions,[7c] the weak binding between the two agents often results in undesired separation upon therapeutic administrations which can significantly hamper the spatially concerted action for synergistic effect. Herein, we report a novel AuNR-based thermo-chemo combination therapy platform with DNA hydrogel (Dgel) (Scheme 1). Dgel is three-dimensional structure composed of internally cross-linked DNA monomers with many nanoscale pores (Scheme 1a).[9] Because the DNA backbone is highly negatively charged, AuNRs which are positively surface-charged can be stably incorporated into the Dgel pores by electrostatic attractions. Dgel is also exploited as a template for small anticancer drug loading. Dgel can be used as a delivery vehicle for DNA-binding anticancer drugs with the strong binding affinity preventing biodegradation or uncontrolled release of the payloads.[9a] Recently, we have reported Dgel-AuNP assembly system for synergistic cancer therapy.[10] Dgel can be a biocompatible scaffold with unique melting characteristics by the thermal denaturation, which can be taken advantage for triggered drug release and/or programmed disassembly after therapy (Scheme 1b). The Dgel platform with NIR-responsive AuNRs and DNA-binding anticancer drugs allows stable NR and drug loadings and 'on-demand' type activation of the therapeutic combination action by external light triggering. AuNR incorporation, suggesting that the AuNR loading does not severely perturb the DNA stacking backbones in the Dgel.

Positively charged AuNRs (length 35.6 (±2.6) nm, width 20.9 (±9.9) nm) were prepared by following a seedless growth method described in the literature (See Fig. 1a for the TEM image).[11] Excess free CTAB in the AuNR solution was rigorously removed by centrifugations and decantings. X-shaped DNA (X-DNA) was

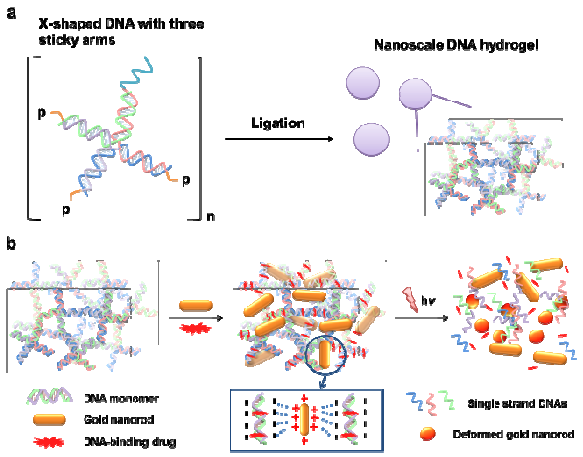

Scheme 1. (a) Schematic drawing of Dgel nanoscaffold synthesis. The X-DNAs with one disabled arm (left) are mixed and ligated to produce nanoscale Dgel (right). (b) Schematic illustration of DNA gel, gold nanorod incorporation, and cancer drug loading. External light triggering induces the drug release by DNA melting, which permits synergistic thermo-chemo combination cancer therapy.

Table 1. Sequence design for X-DNA building block [a]

Strand	End segment	Main body segment
X01	5'-p-ACGT[a]	CGA CCG ATG AAT AGC GGT CAG ATC CGT ACC TAC TCG-3'
X02	5'-p-ACGT	CGA GTA GGT ACG GAT CTG CGT ATT GCG AAC GAC TCG-3'
X03	5'-p-ACGT	CGA GTC GTT CGC AAT ACG GCT GTA CGT ATG GTC TCG-3'
X04	5'-$(GT)_{20}$	CGA GAC CAT ACG TAC AGC ACC GCT ATT CAT CGG TCG-3'

[a] 5'-p represents the phospholylated 5' end of oligonucleotide

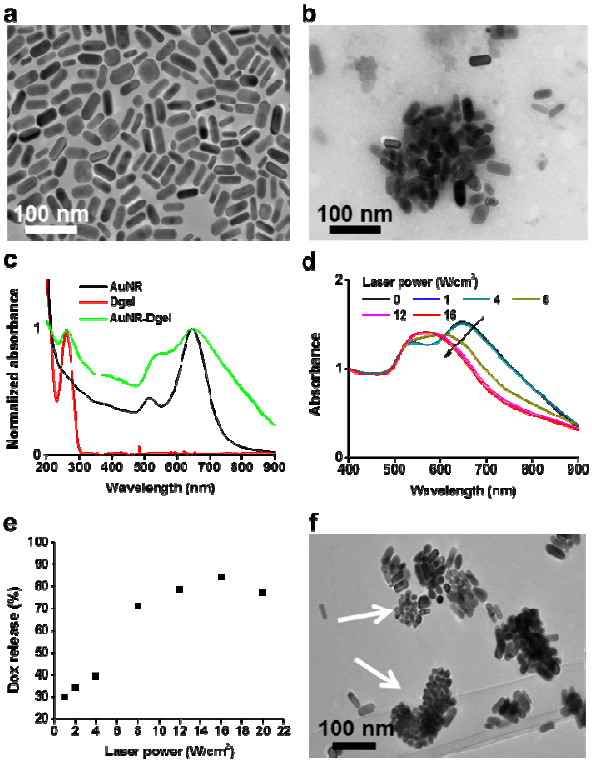

Fig. 1. TEM images of AuNR (a) and AuNR-Dgel (b). (c) Absorption spectra of AuNR, Dgel, and AuNR-Dgel. Laser power dependent absorption spectra (d) and Dox release percentages (e) of Dox-AuNR-Dgel upon the irradiations for 5 mins. (f) TEM image of Dox-AuNR-Dgel after the laser irradiation at 16 W/cm^2 for 5 mins.

designed to have three sticky hands and one disabled end to control the size of Dgel upon ligation (Scheme 1a, Table 1). The self-confined geometry by the disabled arm has provided the control over the crosslinking and thus yielded Dgels around one hundred nanometers in size. In the case of X-DNA with all four sticky hands, the enzymatic crosslinking resulted in bulk Dgels of over microns in size. In the case of X-DNA with all four sticky hands, the enzymatic crosslinking resulted in bulk Dgels of over microns in size. Freezing dried Dgel was swelled under AuNR aqueous solution. Then, the mixture was centrifuged to remove unassembled free Dgels and AuNRs. AuNR incorporated Dgel (AuNR-Dgel) was prepared by mixing Dgels with AuNRs in deionized water. When a Dgel sample prepared by the ligation of 10 nmol X-DNA was co-incubated with 2.5 pmol AuNR, near complete incorporation was confirmed spectrophotometrically by the absence of free AuNR in the supernatant after centrifugation. The Dgel retained the colloidal stability after the AuNR loading. TEM measurement showed tens to hundreds of AuNRs densely incorporated into a Dgel (Fig. 1b). Average hydrodynamic (HD) sizes determined by dynamic light scattering were 32 (±14) nm for AuNR, 87 (±6) nm for Dgel, and 148 (±67) nm for AuNR-Dgel, respectively (Fig. S1). The HD increase of Dgel upon AuNR loading suggests partial inclusion of AuNRs in the Dgel, which is quite expected when considering the significant size of AuNR to Dgel. This was supported by the partial charge compensation of the Dgel upon AuNR incorporation. The Dgel initially showed the Zeta potential of -46 mV which reduced (in absolute value) to -27 mV upon the incorporation of AuNR of which Zeta potential was 34 mV (Fig. S2). Fig. 1c shows the absorption profiles of AuNR, Dgel, and AuNR-Dgel. AuNR initially shows two distinct plasmon peaks at 515 and 650 nm which correspond to the transverse and longitudinal modes, respectively. Upon the incorporation into Dgel, AuNR showed broadened and red-shifted plasmon peaks. The transverse peak showed ~20 nm red-shift, whereas the longitudinal peak did not show much shift although it manifested the noticeable tailing to the long wavelength. It has been reported by others that a side-by-side assemblies of eight AuNRs (which showed the similar aspect ratio as what we have used in this paper) resulted in 20 nm transverse peak shift.[12] The larger red-shift of transverse peak over longitudinal peak is presumably due to dominant side-by-side plasmon couplings between AuNRs inside Dgel. The DNA peak at 260 nm remained unchanged after the AuNR incorporation, suggesting that the AuNR loading does not severely perturb the DNA stacking backbones in the Dgel.

The high-density DNA strands of Dgel was taken advantage to co-load a DNA binding drug. To obtain doxorubicin (Dox) and AuNR co-loaded Dgel (Dox-AuNR-Dgel), Dox was co-incubated 1 h with AuNR-Dgel in deionized water and unloaded free Dox was removed by centrifugation. The amounts of loaded Dox (by subtracting unloaded Dox from the co-incubated Dox) and the number of AuNRs in the AuNR-Dgel sample were obtained by the spectrophotometric method using the extinction coefficients reported elsewhere.[13] On average, 11,000 Dox molecules were loaded per AuNR (Fig. S3). Upon the earlier hypothesis of one million X-DNAs constructing a Dgel, each Dox-AuNR-Dgel is co-loaded with 250 AuNRs and 2.8 million Dox molecules which corresponds to 2.8 Dox molecules being incorporated into each X-DNA building block.

Dox-AuNR-Dgel is designed for the light-triggered release of Dox by the plasmonic heat shock. To test if Dox can be released upon photothermally-triggered DNA melting, 660 nm laser which matches the major plasmonic peak of the AuNR was irradiated to Dox-AuNR-Dgel samples at different laser power densities for 5 min each. As the laser power increased, the absorption blue-shifted progressively. The longitudinal peak of the AuNR shifted abruptly above 8 W/cm^2, which can be described that AuNRs generated sufficient energy to melt the Dgel (Fig. 1d).[14] This also accords with the drastically increased Dox release at or above 8 W/cm^2 laser power (Fig. 1e). The amount of Dox released by the light-triggering was investigated by the supernatant absorption measurements after centrifugations. Linear increase by the laser power up to 16 W/cm^2 followed by plateauing was observed (Fig. 1e, Fig. S4). Efficient Dox release was demonstrated with the percentage as high as 85%. TEM measurements show fragmentation of the Dgel template and shape transformations of AuNRs into more spherical particles (Fig. 1f). Such AuNR shape deformation is known to occur at the local temperature above 200 °C,[14] which explains well the efficient DNA melting and subsequent Dox release. At the nearby, a complete release of Doxs from Dgel is expected as the Dgel turns into single strands above the melting temperature from the Dox intercalated B-form of the DNA double stranded helix.[15]

The successful demonstration of light-triggered release of heat shock and Dox allowed us to investigate cellular level combination

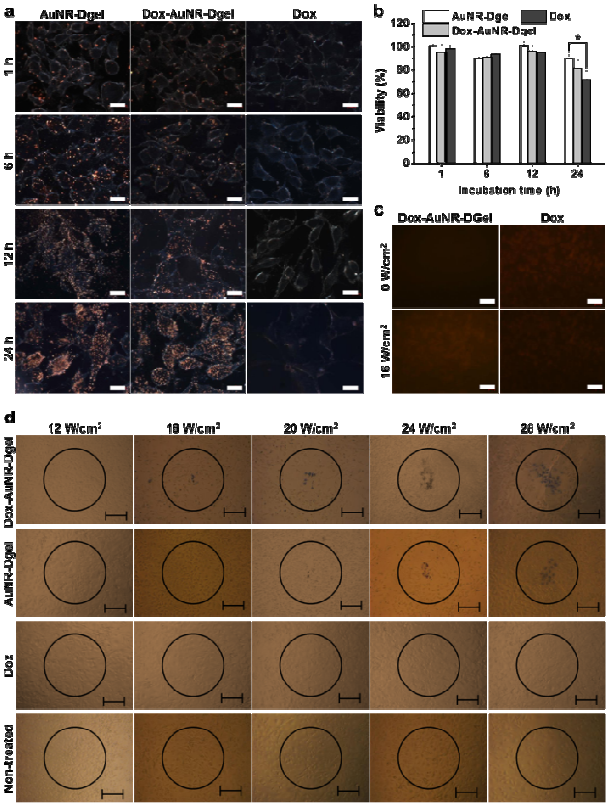

Fig. 2. (a) Dark field microscope images of B16 F10 cells co-incubated with AuNR-Dgel, Dox-AuNR-Dgel, or Dox for 1, 6, 12, or 24 h (scale bar: 20 μm). (b) Viabilities of the B16 F10 cells co-incubated with each sample for 1, 6, 12 or 24 h. ($^{*}P$ = 0.019). (c) Fluorescence microscope images B16 F10 cells co-incubated with Dox-AuNR-Dgel or with Dox and irradiated with no laser (0 W/cm^2) or with laser power of 16 W/cm^2. (scale bar: 40 μm). (d) Photothermal destruction of the cells co-incubated with Dox-AuNR-Dgel, AuNR-Dgel, Dox, or no sample (non-treated) for 12 h followed by laser irradiation for 5 min at different power densities (scale bar: 100 μm).

cancer therapy. B16 F10 cells were incubated with Dox-AuNR-Dgel which had been prepared by the ligation of 0.24 nmol X-DNA and subsequent co-loading of 0.06 pmol AuNR and 0.03 nmol Dox. The controls of AuNR-Dgel and Dox only were also prepared using identical concentrations. Cellular accumulations of AuNRs were monitored over time using dark-field microscopy. Dox-AuNR-Dgel and AuNR-Dgel showed similar accumulations over time as indicated by the increased orange-color scatterings visualizing the cell morphologies (Fig. 2a). Cell viabilities were also measured over time by MTT assay. Under no laser light, no significant cytotoxicity was observed up to 12 h for all the cases (Fig. 2b). At 24 h, slight cytotoxicity was observed for the Dox only control. Light-triggered release of Dox was confirmed by the appearance of Dox red fluorescence as recovering from the quenched state in Dox-AuNR-Dgel (Fig. 2c). Quantitative measurements for the fluorescence can be found in Fig. S5. Since internalization of the Dox-AuNR-Dgel and Dox release were confirmed, we further performed the thermo-chemo combination cancer therapy. The co-incubation conditions used for dark-field microscopy and MTT assays were adopted, and 660 nm laser was used for illumination. Circles in Fig. 2d represent the position of 660 nm laser spots. The spot has a ~500 μm radius, as is measured using photosensitive paper. Each sample was illuminated for 5 min using different laser power densities of 12, 16, 20, 24, and 28 W/cm^2. Trypan blue was used to reveal the mortality of cells with blue staining. In the case of Dox-AuNR-Dgel, mortal cells appeared at a laser power of 16 W/cm^2 or higher. The circular

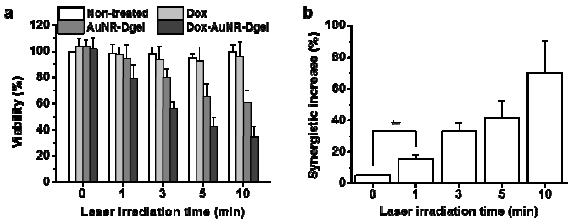

Fig. 3. (a) Viabilities of cells co-incubated with each or no sample and exposed to laser irradiations. (b) Synergistic effects for the Dox-AuNR-Dgel. ($^{**}P$ = 0.0039).

areas of damaged cells increased linearly with the irradiation power density. AuNR-Dgel showed significantly larger threshold, showing the mortality at 20 W/cm^2 or higher. On the other hand, no noticeable mortal cells were found for the controls of Dox and Non-treated. It is noted that the cells outside of the laser spot also showed no mortality. As the Dox release concurrently burst with the heat shock, the thermo and chemo effects boosted each other. This synergistic effect has resulted in the reduction of laser threshold for Dox-AuNR-Dgel over AuNR-Dgel. Conversely, this combination therapy would require less amount of Dox than the uncombined case. The synergistic effect can potentially mitigate the side effect of patients by reducing the dosage (or laser power).

To quantify the synergistic effect, viabilities were studied for cells co-incubated with Dox-AuNR-Dgel and separately with the AuNR-Dgel, Dox only, and non-treated controls for 12 h as varying the laser irradiation time from 0 (no exposure), 1, 3, 5, to 10 min at 16 W/cm^2 (Fig. 3a). Dox-AuNR-Dgel showed the most radical change in the viability by the irradiation time, dropping to 34.2% at 10 min, which was followed by AuNR-Dgel showing 60.5% viability at the same irradiation condition. This almost two-fold viability reduction of Dox-AuNR-Dgel over AuNR-Dgel indicates the highly synergistic effect by the co-loaded Dox. It is noted that the Dox alone only showed ~4% decrease in the viability because of the low dosage level. Synergistic effects were obtained by dividing the predicted additive viability by the measured viability (Fig. 3b).[8] The additive viability was obtained from the expression $V_{Additive} = V_{Chemo} \times V_{Thermo}$, where $V_{Additive}$ is the predicted viability as a result of the purely additive interaction between the chemo and thermo therapies, and V_{Chemo} and V_{Thermo} are the viabilities after the chemo and thermo therapies alone, respectively.[7a, 16] The synergistic factor was ~1 for all the samples prior to laser irradiation, which indicates the absence of any synergistic effect. The largest synergistic increase of 70.0% was observed for Dox-AuNR-Dgel sample after 10 min laser irradiation. The synergistic factor is comparable with maximal values observed for previous combination treatments using gold nanostructures with Dox.[7c, 17] The highly synergistic effect of Dox-AuNR-Dgel can be explained by 1) high local concentration of Dox released from the Dgel scaffold by thermal denaturation and 2) photothermally enhanced induction of the cytotoxic effect of Dox, i.e., thermal chemopotentiation.[18]

The efficacy of combination therapy was further demonstrated in vivo using a mouse model bearing B16 F10 melanoma xenografts. PBS buffer, Dox, AuNR-Dgel, or Dox-AuNR-Dgel was intratumorally injected, and the tumor growth was monitored with/without laser irradiations. To monitor the local heating effect, a thermocouple needle was inserted into the tumor region 10 min post injection, and the local temperature was measured for 5 min during irradiation under 660 nm laser (1 W/cm^2) and for another 3 min after the laser turned off (Fig. 4a). Both AuNR-Dgel and Dox-AuNR-Dgel showed rapid temperature increase upon laser, which was significantly larger than that of PBS or Dox control. This temperature increase should be sufficient for tumor ablation[19] and

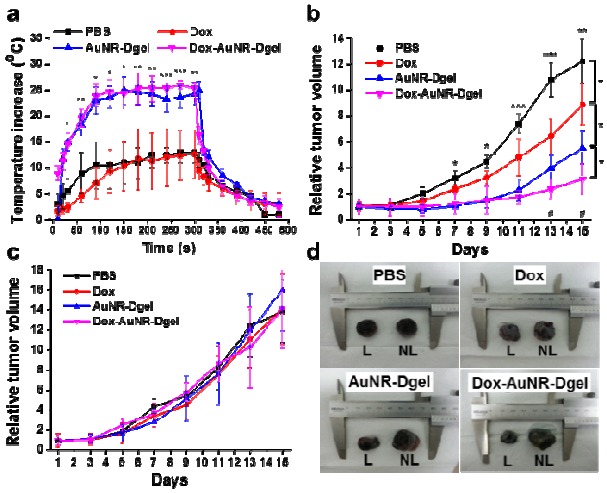

Fig. 4. (a) Local temperature of the tumor core during and after laser irradiations at 10 min after injection of PBS, Dox, AuNR-Dgel, or Dox-AuNR-Dgel ($^{*}P < 0.05$ and $^{**}P < 0.005$ for comparison with Dox and PBS). Relative tumor volume change over 15 days with (b) or without (c) laser irradiation ($^{*}P < 0.05$, $^{**}P < 0.005$ and $^{***}P < 0.001$ are noted between PBS and Dox-AuNR-Dgel, $^{\#}P < 0.05$ is noted between AuNR-Dgel and Dox-AuNR-Dgel). (d) Images of dissected tumors after the experiment with laser irradiation (L) or without (NL) laser irradiation.

thermal enhancement of Dox cytotoxicity.[18, 20] As the laser turned off, the tumor quickly cooled down, implying that the heat generation was localized. After the intratumoral administrations, the mice were laser-irradiated only once for 5 min on the day one. Tumor suppression efficacy was evaluated by recording the relative tumour volumes by every two days for two weeks (Fig. 4b). Dox-AuNR-Dgel treated mice showed the most effective tumor suppression, which was followed by AuNR-Dgel and Dox. The Dox-AuNR-Dgel case showed the relative tumor volume that was 3.9 times smaller than the PBS control. It was also 1.8 times and 2.9 times smaller than those of the AuNR-Dgel and Dox, respectively, which clearly indicates the synergistic effect. The experiment was repeated as omitting the laser irradiation, where no significant tumor suppression was observed (Fig. 4c). The tumors were dissected after the experiments, and showed well-correlated size patterns with the temporal volume change (Fig. 4d). The dissected tumors were measured and compared by weight, which matched well with the volume data on the last day (Fig. S6). These results demonstrate light-controlled activation of thermo-chemo combination therapy, which shows synergistically enhanced efficiency over single treatment.

In summary, to overcome the limited conjugation capability of AuNRs, we have employed Dgel as a scaffold to assemble AuNRs with Doxs in nanoscale proximity. This platform can be potentially applied for CT imaging contrast, radiosensitization, and so forth.

Acknowledgement

This research was supported by Korea Health Technology R&D Project through KHIDI (HI12C1642) and by National R&D Program for Cancer Control (1320220), Ministry for Health and Welfare, Republic of Korea.

Notes and references

[a] School of Interdisciplinary Bioscience and Bioengineering, Pohang University of Science & Technology (POSTECH), San 31, Hyojadong, Pohang 790-784, Korea, E-mail:sungjee@postech.ac.kr; Tel:82-54-279-2108
[b] Samsung Advanced Institute of Technology, Samsung Electronics, Yongin, Gyeonggi-do, 446-712, Korea.
[c] Department of Chemistry, POSTECH, Korea.
[d] Department of Chemical and Biological Engineering, Gachon University, Seongnam, Gyeonggi-do, 461-701, Korea
[e] Division of Integrative Biosciences and Biotechnology, POSTECH, Korea.
[f] Department of Chemistry, Myongji University, Yongin, Gyeonggi-do 449-728, Korea. E-mail: pospnk@mju.ac.kr Tel: +82-31-330-6188
Electronic Supplementary Information (ESI) available: [Experimental section and supplementary figures]. See DOI: 10.1039/c000000x/

1 P. K. Jain, X. Huang, I. H. El-Sayed and M. A. El-Sayed, *Acc. Chem. Res.*, 2008, **41**, 1578.
2 (a) W. I. Choi, J. Y. Kim, C. Kang, C. C. Byeon, Y. H. Kim and G. Tee, *Acs Nano*, 2011, **5**, 1995; (b) G. von Maltzahn, A. Centrone, J.-H. Park, R. Ramanathan, M. J. Sailor, T. A. Hatton and S. N. Bhatia, *Adv. Mater.*, 2009, **21**, 3175; (c) X. Huang, I. H. El-Sayed, W. Qian and M. A. El-Sayed, *J. Am. Chem. Soc.*, 2006, **128**, 2115.
3 (a) C. Loo, A. Lowery, N. Halas, J. West and R. Drezek, *Nano Lett.*, 2005, **5**, 709; (b) L. R. Hirsch, R. J. Stafford, J. A. Bankson, S. R. Sershen, B. Rivera, R. E. Price, J. D. Hazle, N. J. Halas and J. L. West, *P Natl Acad Sci USA*, 2003, **100**, 13549.
4 (a) S. E. Skrabalak, J. Chen, Y. Sun, X. Lu, L. Au, C. M. Cobley and Y. Xia, *Acc. Chem. Res.*, 2008, **41**, 1587; (b) L. Au, D. Zheng, F. Zhou, Z.-Y. Li, X. Li and Y. Xia, *Acs Nano*, 2008, **2**, 1645.
5 C. Sonnichsen, B. M. Reinhard, J. Liphardt and A. P. Alivisatos, *Nat Biotech*, 2005, **23**, 741.
6 (a) E. S. Shibua, M. Hamadaa, N. Murasea, V. Biju, *J. Photochem. Photobiol. C: Photochem. Rev.* 2013, **15**, 53; (b) J. Nam, N. Won, J. Bang, H. Jin, J. Park, S. Jung, S. Jung, Y. Park and S. Kim, *Adv. Drug Delivery Rev.*, 2013, **65**, 622.
7 (a) T. S. Hauck, T. L. Jennings, T. Yatsenko, J. C. Kumaradas and W. C. W. Chan, *Adv. Mater.*, 2008, **20**, 3832; (b) J.-H. Park, G. von Maltzahn, M. J. Xu, V. Fogal, V. R. Kotamraju, E. Ruoslahti, S. N. Bhatia and M. J. Sailor, *Proc. Natl. Acad. Sci. U.S.A.*, 2010, **107**, 981; (c) H. Park, J. Yang, J. Lee, S. Haam, I.-H. Choi and K.-H. Yoo, *Acs Nano*, 2009, **3**, 2919.
8 J. Nam, W.-G. La, S. Hwang, Y. S. Ha, N. Park, N. Won, S. Jung, S. H. Bhang, Y.-J. Ma and Y.-M. Cho, *Acs Nano*, 2013, **7**, 3388.
9 (a) S. H. Um, J. B. Lee, N. Park, S. Y. Kwon, C. C. Umbach and D. Luo, *Nat. Mater.*, 2006, **5**, 797; (b) J. B. Lee, S. Peng, D. Yang, Y. H. Roh, H. Funabashi, N. Park, E. J. Rice, L. Chen, R. Long and M. Wu, *Nat. Nanotechnol.*, 2012, **7**, 816.
10 J. Song, S. Hwang, K. Im, J. Hur, J. Nam, S. Hwang, G. O. Ahn, S. Kim and N. Park, *J. Mater. Chem. B*, 2015, **3**, 1537.
11 P. Zijlstra, C. Bullen, J. W. M. Chon and M. Gu, *J. Phys. Chem. B*, 2006, **110**, 19315.
12 (a) W. Ma, H. Kuang, L. Xu, L. Ding, C. Xu, L. Wang and N. A. Kotov, *Nat. commun.*, 2013, **4**; (b) L. Wang, Y. Zhu, L. Xu, W. Chen, H. Kuang, L. Liu, A. Agarwal, C. Xu and N. A. Kotov, *Angew. Chem. Int. Ed.*, 2010, **49**, 5472.
13 C. J. Orendorff and C. J. Murphy, *J. Phys. Chem. B*, 2006, **110**, 3990.
14 H. Petrova, J. Perez Juste, I. Pastoriza-Santos, G. V. Hartland, L. M. Liz-Marzan and P. Mulvaney, *Phys. Chem. Chem. Phys.*, 2006, **8**, 814.
15 (a) C. A. Frederick, L. D. Williams, G. Ughetto, G. A. Van der Marel, J. H. Van Boom, A. Rich and A. H. Wang, *Biochemistry*, 1990, **29**, 2538; (b) O. Tacar, P. Sriamornsak and C. R. Dass, *J. Pharm. Pharmacol.*, 2013, **65**, 157; (c) J. B. Lee, A. S. Shai, M. J. Campolongo, N. Park and D. Luo, *ChemPhysChem*, 2010, **11**, 2081.
16 G. M. Hahn, J. Braun and I. Har-Kedar, *P Natl Acad Sci USA*, 1975, **72**, 937.
17 J. You, G. Zhang and C. Li, *Acs Nano*, 2010, **4**, 1033.
18 (a) P. Jacquet, A. Averbach, O. A. Stuart, D. Chang and P. H. Sugarbaker, *Cancer Chemother. Pharmacol.*, 1997, **41**, 147; (b) P. Wust, B. Hildebrandt, G. Sreenivasa, B. Rau, J. Gellermann, H. Riess, R. Felix and P. M. Schlag, *Lancet Oncol.*, 2002, **3**, 487.
19 (a) S. M. Lee, H. Park and K. H. Yoo, *Adv. Mater.*, 2010, **22**, 4049; (b) E. B. Dickerson, E. C. Dreaden, X. Huang, I. H. El-Sayed, H. Chu, S. Pushpanketh, J. F. McDonald and M. A. El-Sayed, *Cancer Lett.*, 2008, **269**, 57.
20 J. M. C. Bull, *Cancer Res.*, 1984, **44**, 4853.

The table of contents entry:
The drug delivery vehicle have been prepared by combining gold nanorod and DNA intercalated drug in DNA hydrogel, resulting in thermo chemo combiation therapy with photothermal-triggered DNA melting and release of Doxorubicin.